CrossMark

ORIGINAL PAPER

Correlating Molecular Structure to the Behavior of Linear Styrene–Butadiene Viscosity Modifiers

Uma Shantini Ramasamy[1] · Michelle Len[1] · Ashlie Martini[1]

Abstract The effect of linear styrene–butadiene polymer structure on the temperature–viscosity behavior of model polymer-base oil solutions is investigated using molecular dynamics simulations. Simulations of alternating, random, and block styrene–butadiene polymers in a dodecane solvent are used to calculate viscosity at 40 and 100 °C, reference temperatures for characterizing their function as viscosity modifiers. Mechanisms underlying this function are explored by quantifying the radius of gyration and intramolecular interactions of the polymers at the same reference temperatures. The block styrene–butadiene configuration exhibits the least change in viscosity with temperature, characteristic of a good viscosity modifier or viscosity index improver, and the behavior is correlated to the ability of this structure to form smaller coils with more intramolecular interactions at lower temperatures and then expand as temperature is increased. The results indicate that there is a correlation between styrene–butadiene polymer structure, additive function, and the mechanisms underlying that function.

Keywords Viscosity modifiers · Viscosity index improver · Styrene–butadiene · Radius of gyration · Intramolecular interactions

✉ Ashlie Martini
amartini@ucmerced.edu

[1] School of Engineering, University of California Merced, Merced, CA, USA

1 Introduction

Viscosity, a fluid property that resists flow, is an important characteristic of lubricating oils. In machines, fluid viscosity drives the formation and strength of lubricating films and ultimately determines the success or failure of a lubricated component. A significant change in oil viscosity can result in increased friction, heat generation, and wear. Therefore, it is vital for a lubricant's viscosity to change minimally with fluctuating operating conditions. The temperature–viscosity response of a lubricant can be controlled by the addition of specific high molecular weight polymers known as viscosity modifiers (VM)s. Commonly used VM chemistries are olefin copolymers, polyalkylmethacrylates, polyisobutylenes, and styrene block copolymers. Some of these additives increase the viscosity index of the fluid and so are called viscosity index improvers (VII). At optimum concentrations, the polymers can minimize changes in fluid viscosity with temperature and increase the load bearing capability of the lubricating oil [1, 2].

Current advancements in VII technology focus on modifying chemistries [3–5] and molecular architecture [6–8] to improve the functionality of traditional VII polymers. These variations not only improve the viscosity index of the lubricant, but in some cases also reduce friction and boost shear, thermal, and oxidative stability of the lubricating oil [3, 7–11]. Several authors have explored the influence of molecular structure, architecture, and chemical features on the temperature–viscosity behavior of fluids using experimental methods [12–15, 17] and molecular simulation tools [16–18]. Some of the features investigated include the effects of isomers [16], chain architecture (linear, comb, star) [12, 13, 17, 18], variation in moieties [15], as well as the nature and configuration of double

Springer

bonds [14]. Overall, these studies reveal that diversity at the molecular level can impact the temperature–viscosity response of a fluid.

Recent research has also focused on the mechanisms by which polymers improve the temperature–viscosity response of fluids. The most commonly studied mechanism is coil expansion, in which polymers expand with temperature and therefore impede fluid flow, i.e., increase viscosity more at higher temperatures [19, 20]. This behavior has been observed experimentally for some, but not all, VM polymers [17, 19, 21–23]. The coil expansion mechanism has also recently been studied using molecular dynamics (MD) simulations [17, 24]. MD is an ideal tool to characterize such mechanisms since the positions and trajectories of all the atoms in the system are known.

In this study, we investigate the effects of linear styrene–butadiene polymer structure on VII performance using MD simulation. Styrene–butadiene is chosen for this work because it was one of the first polymers to be used as a VII additive and has been extensively studied. Additionally, a linear architecture is chosen for simplicity. Styrene–butadiene polymers with alternating, random, and block structures in a dodecane base fluid are characterized in terms of their viscosity–temperature behavior and mechanisms underlying that behavior. First, viscosity is calculated for each configuration and performance is characterized in terms of the rate of change of viscosity as temperature is increased from 40 to 100 °C. Then, mechanisms are explored by quantifying the radius of gyration and the number of intramolecular contact pairs of each polymer model as functions of temperature. Lastly, the trends in coil size and intramolecular contact are correlated with the temperature–viscosity behavior. The results indicate that structural properties affect the response of the polymer to temperature and therefore may be used to optimize additive function, i.e., minimize the decrease in solution viscosity with temperature.

2 Methods

Linear styrene–butadiene (SB) polymers with three different configurations, alternating (ALT), random (RDM), and block (BLK), are modeled in this work. Figure 1 shows a conceptual schematic of the three SB configurations. All three configurations are 50 repeat units in length, where the ALT and RDM structures have 25:25 styrene–butadiene ratios (3958 g/mol), while the BLK structure has 26:24 styrene–butadiene ratio (3994 g/mol). Illustrations of the styrene and butadiene monomers are shown in Fig. 2a. All polymers are diluted in a dodecane solvent. Due to the size- and time-scale limitations of the MD methodology, the molecular weights of the polymers used in this
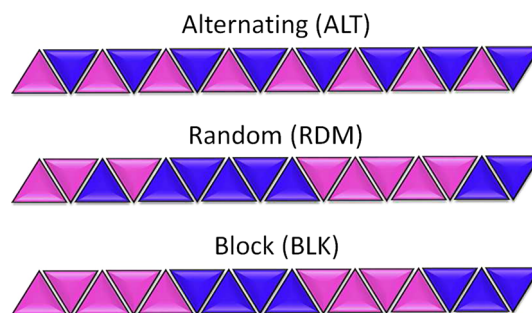
Fig. 1 Schematic representations of the three configurations modeled, where the pink triangles represent styrene monomers and the blue triangles represent butadiene monomers (Color figure online)
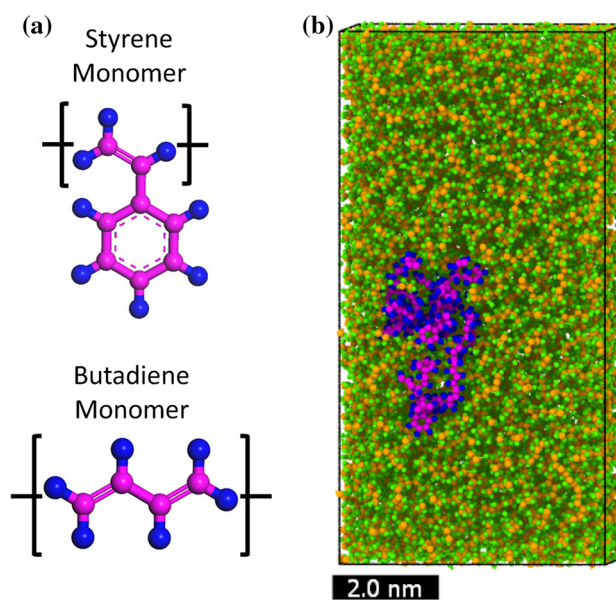
Fig. 2 a Illustrations of the styrene and butadiene monomers that comprise all three SB configurations. b Initial structure of the BLK styrene–butadiene configuration in dodecane solvent used in simulations for calculating viscosity. Each simulation model consists of one polymer molecule and 684 dodecane molecules to maintain a 3.3% (w/w) concentration. The dodecane solvent is represented by orange (carbon) and green (hydrogen) spheres, while the BLK polymer is represented by pink (carbon) and blue (hydrogen) spheres (Color figure online)

investigation are smaller than realistic additive molecules, which will result in lower solution viscosities. However, we expect the trends in viscosity, coil expansion, and intramolecular interactions observed with the small model polymer solution reported here will be consistent with those exhibited by solutions with larger polymeric additives.

Simulation models are created by placing one polymer in a dodecane solvent using Accelrys Materials Studio and then implementing dynamics with Large Atomic/Molecular Massively Parallel Simulation (LAMMPS) software [25]. The concentration of polymer in each solution is maintained at 3.3% (w/w). The All Atom Optimized

Potentials for Liquid Simulations (OPLS-AA) force field [26] with a global cutoff of 1.2 nm is used to describe bond, angle, torsion, and non-bonded interactions between all atoms. A long range solver is not used in this work. A Nosé-Hoover thermostat and barostat with relaxation time constants of 100 and 1000 fs, respectively, are used to control temperature and pressure [27–29]. All simulations are run with a time step of 1.0 fs and a 1–4 intramolecular van der Waals scaling factor of 0.0. This scaling factor has been shown to increase the accuracy of density predictions for molecules with more than 12 carbon atoms [30]. The initial configurations are relaxed under NVT conditions (constant number of atoms, volume, and temperature) at high temperature (727 °C) for 0.5 ns, before being equilibrated under NPT conditions (constant number of atoms, pressure, and temperature) at 1 atm at both 40 and 100°C for 2–3 ns.

2.1 Viscosity

Viscosity simulations are implemented using a periodic simulation box with initial dimensions of 5.0 nm × 5.0 nm × 10.0 nm for the SB in dodecane systems and 3.0 nm × 3.0 nm × 6.0 nm for the pure dodecane system. Figure 2b depicts the simulation model used to calculate viscosity for the BLK configuration; models for the other configurations look similar. After the initial relaxation and equilibration process, these structures are further equilibrated under NVT conditions at 40 and 100°C for 0.5 ns.

Viscosity calculations are then implemented using the reverse non-equilibrium molecular dynamics (RNEMD) technique [31, 32]. The RNEMD technique exchanges momenta between two atoms in different regions of the simulation box. For all cases, momenta is only exchanged between solvent molecules. The momenta exchange imposes a momentum flux onto the simulation box and the system responds by producing a shear velocity profile. The momentum flux, $j_z(p_x)$, and the shear rate (slope of the shear velocity profile), $\frac{\partial v_x}{\partial z}$, are used to estimate shear viscosity, η, where $\eta = -j_z(p_x)/\frac{\partial v_x}{\partial z}$. RNEMD simulations are run at 40 and 100 °C at a range of shear rates.

Viscosity simulations are run at various shear rates for a total of 12 ns, which includes 4 ns of equilibration and 8 ns of data collection. Reported viscosities are averaged over the last 1 ns of simulation time. Newtonian viscosity is then extrapolated from the viscosity vs. shear rate plot using the following Carreau model [33]

$$\eta(\dot{\gamma}) = \frac{\eta_0}{\left[1 + (\lambda\dot{\gamma})^2\right]^p} \tag{1}$$

where $\eta(\dot{\gamma})$ is shear viscosity, η_0 is Newtonian viscosity, λ is relaxation time, $\dot{\gamma}$ is shear rate, and p is the power index.

2.2 Radius of Gyration

For all three SB configurations, the radius of gyration of the polymers is calculated from periodic models with an initial size of 6.0 nm × 6.0 nm × 6.0 nm. The production phase begins after the initial relaxation and equilibration process. During the production phase, the system continues to run under NPT conditions at 40 and 100°C for 100 ns. During that time, the polymer's radius of gyration, R_g, is calculated and used to quantify the size of the polymer coil. In MD simulations, R_g is defined as the mass weighted average distance from the center of mass of the molecule to each atom in the molecule

$$R_g = \sqrt{\frac{1}{M}\sum_i m_i(r_i - r_{cm})^2} \tag{2}$$

where M is the total mass of the molecule, m_i is the mass of atom i, r_i is the position of atom i, and r_{cm} is the center of mass of the molecule.

During the production simulation, the polymer's R_g is calculated every 5 ps. The instantaneous R_g is used to plot frequency histograms that capture the recurrence of specific conformations throughout the simulation duration. Next, a Gaussian function is fit to the frequency histogram to quantify the mean, μ, and skewness of the distribution. The percent change in coil size with temperature, for all three configurations, is calculated from the mean of the distribution using $(\mu_{100\,°C} - \mu_{40\,°C})/\mu_{40\,°C} \times 100$ [24].

2.3 Intramolecular Interactions

Interactions between atoms within each polymer are characterized to provide additional information about the effect of temperature on polymer structure. A method for quantifying intramolecular interactions is developed that calculates the distance between every two carbon atoms in the polymer backbone and identifies contact pairs as atoms whose distance from one another is within a specified cutoff radius. This approach is based on the concept of atom contact used for nanoscale junctions between solids [34]. In this study, the cutoff radius is specified as 4.62 Å, which is three times the length of a carbon–carbon covalent bond and is the minimum distance required to capture contacts that occur due to intramolecular interactions. If the cutoff distance is any smaller, then the method captures only contacts that occur between neighboring carbons in the chain and not intramolecular interactions within the coil.

The number of contact pairs for a given configuration is dependent on the cutoff and so is not meaningful by itself. However, the difference between the number of contact pairs in the coiled and uncoiled states effectively captures

the degree of contact due to coiling. Therefore, the contact pair calculations are first performed on reference cases, which are models of uncoiled or elongated SB polymers. For the reference state, a single elongated polymer in a simulation box is created in Materials Studio and read into LAMMPS for minimization and NVT equilibration at 40 and 100°C for 5000 fs. The reference contact pair analysis is performed after initial relaxation (after 700 fs) and before the polymer coils up (before 1000 fs). Next, the analysis is performed for the coiled polymers in solution during the production stage of the radius of gyration simulations at 40 and 100°C. The difference in the number of contact pairs for the coiled and the uncoiled reference polymers is reported.

3 Results and Discussion

Figure 3 shows MD shear viscosity results for the dodecane and the dodecane with the three SB configurations at 40 and 100°C. The Carreau equation, Eq. 1, is fit to the MD shear viscosity data to calculate the Newtonian viscosity, η_0, as illustrated by the dashed lines in Fig. 3. Table 1 summarizes the Newtonian viscosities of the pure dodecane and dodecane with each of the three styrene–butadiene configurations. As expected, the viscosities of all fluids are larger at 40 than 100°C. Also, the viscosities of the SB systems are larger than or comparable to that of the pure dodecane system. It should be noted that the simulations overestimate the viscosity of dodecane; literature reports the viscosity of dodecane to be 1.06 mPa.s at 40 °C and 0.51 mPa.s at 100 °C [35]. This implies that the simulation methodology used here may be overestimating the viscosities of the polymer solutions. However, the overestimation is likely to be comparable for all three SB structures, so the trends observed in comparing the
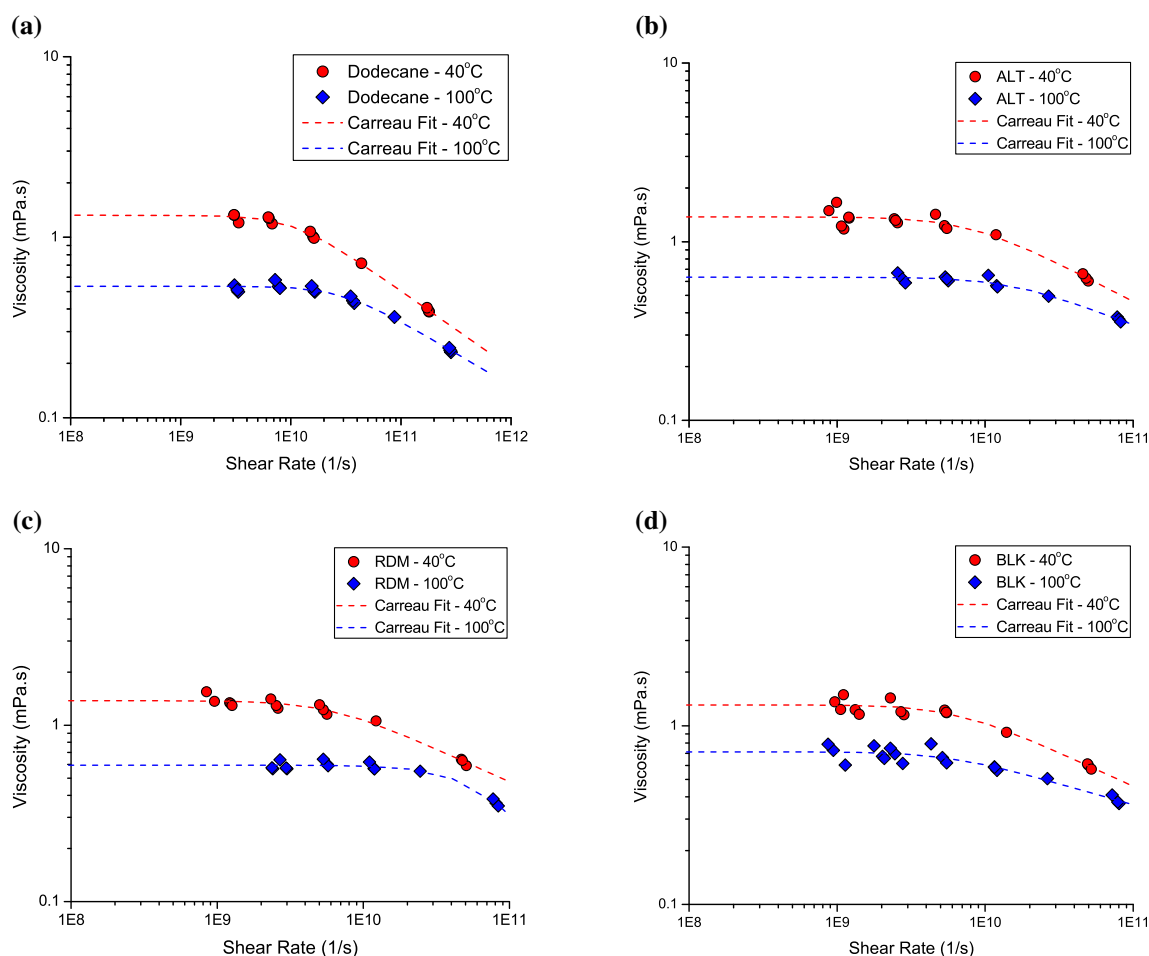
Fig. 3 MD shear viscosity plots for the a dodecane, b ALT, c RDM and d BLK models at 40 and 100 °C. The shear viscosity plots are fit to the Carreau equation to calculate Newtonian viscosity. Overlapping data points are repeat simulations performed under the same conditions but using different seed numbers to generate unique initial velocity distributions

Table 1 Newtonian viscosities for all model systems at 40 and 100°C and the corresponding PVI values

System	$\eta_{40\,°C}$ (mPa.s)	$\eta_{100\,°C}$ (mPa.s)	PVI
Dodecane	1.32 ± 0.03	0.54 ± 0.01	77.5
ALT	1.38 ± 0.05	0.63 ± 0.01	95.6
RDM	1.38 ± 0.03	0.59 ± 0.01	87.0
BLK	1.31 ± 0.04	0.71 ± 0.02	120.6

different models to each other should be accurate and meaningful.

The rate of decrease of a solution's viscosity with temperature is often quantified by its viscosity index, defined per the ASTM D2270 standard. However, our reported $\eta_{100\,°C}$ viscosities are outside the predictive capabilities of that standard, so an alternative metric, the Proportional Viscosity Index (PVI) [36], is used here. This parameter was developed to address some of the limitations of the traditional VI and is defined as $PVI = 2.611 \times (\eta_{100\,°C})^{1.4959} \times 100/\eta_{40\,°C}$, where $\eta_{40\,°C}$ and $\eta_{100\,°C}$ are Newtonian viscosities at $40\,°C$ and $100°C$, respectively. The PVI is calculated from simulation data for dodecane and the three SB configurations. As shown in Table 1, the PVI of all three SB configurations is greater than that of the pure dodecane, with the BLK configuration having the highest PVI.

Fluids with higher PVI values exhibit a smaller decrease in viscosity with temperature. Therefore, the PVI results reported in Table 1 indicate that the BLK configuration has the best temperature–viscosity response of the three configurations studied. The mechanisms underlying the VII performance of SB configurations are explored by analyzing changes in the polymers' radius of gyration and intramolecular interactions over time at both 40 and 100°C.

Radius of gyration is used to quantify the size of the polymer. Instantaneous R_g data are collected at 40 and 100°C, and used to plot frequency histograms that are then fit to a Gaussian distribution. Figure 4a–c shows frequency histograms for the three SB configurations. The mean values of the R_g distributions are reported in Fig. 4d and Table 2. Figure 4d illustrates that the ALT structure has the largest mean R_g while the BLK structure has the smallest mean R_g at both temperatures. These results indicate that the BLK structure is able to form a smaller coil at both temperatures compared to the ALT and RDM configurations. The uncertainties reported in Table 2 are the standard deviations of the Gaussian fit. Large standard deviations indicate that the polymer is able to assume more conformations of different sizes during the simulation.

The percent change in mean R_g with temperature is reported in Table 2. A positive change indicates that the polymer expands while a negative change indicates that the polymer contracts when temperature is increased. Therefore, the positive percent change observed for the BLK configuration suggests that it expands with temperature, while the ALT and RDM configurations either contract or exhibit negligible change in coil size. Table 2 also reports the skewness of the distributions at each temperature. The skewness parameter describes the symmetry of the distribution. A skewness value of zero refers to a distribution with perfect symmetry, and a positive value means a shift to the right, i.e., more conformations with coil sizes larger than the mean value. The BLK configuration shows a significant positive shift in skewness with temperature, implying that the number of large conformations increases with temperature. Overall, the results in Table 2 and Fig. 4b indicate that the BLK configuration has the smallest size and expands the most with temperature.

The ability of the polymers to form coils of various sizes is further analyzed by characterizing their intramolecular interactions. Intramolecular interactions are quantified by estimating the number of carbon-carbon contact pairs present within the polymer backbone at 40 and 100 °C. The results are reported in Table 3, where the uncertainty is the standard deviation. At both temperatures, the BLK configuration has the most contact pairs due to coiling, while ALT SB has the fewest contact pairs. Further analysis reveals that the contact pairs within the BLK configuration at either temperature are primarily attributable to contacts between butadiene monomers. This is consistent with the fact that butadiene chains are more flexible than styrene [37]. Therefore, the BLK structure which contains butadiene blocks is the most flexible and so can form the smallest coils, consistent with the trends in Table 2 where the BLK configuration has the smallest radius of gyration at either temperature.

The viscosity, radius of gyration, and intramolecular interaction investigations reveal that there is a correlation between styrene–butadiene polymer structure, the polymer's response to temperature, and the PVI of the solution. It is observed that the BLK configuration has the best temperature–viscosity response, and this behavior is aided by the ability of the polymer to assume a small and tight coil size at lower temperatures and expand as temperature is increased. Conversely, the ALT and RDM structures, which exhibit smaller PVI than the BLK polymer, have large coil sizes at $40\,°C$ with fewer intramolecular contacts and are not able to expand as temperature is increased to $100\,°C$. These findings imply that SB polymers that are able to form small coils at lower temperatures and then expand with increased temperature may exhibit smaller
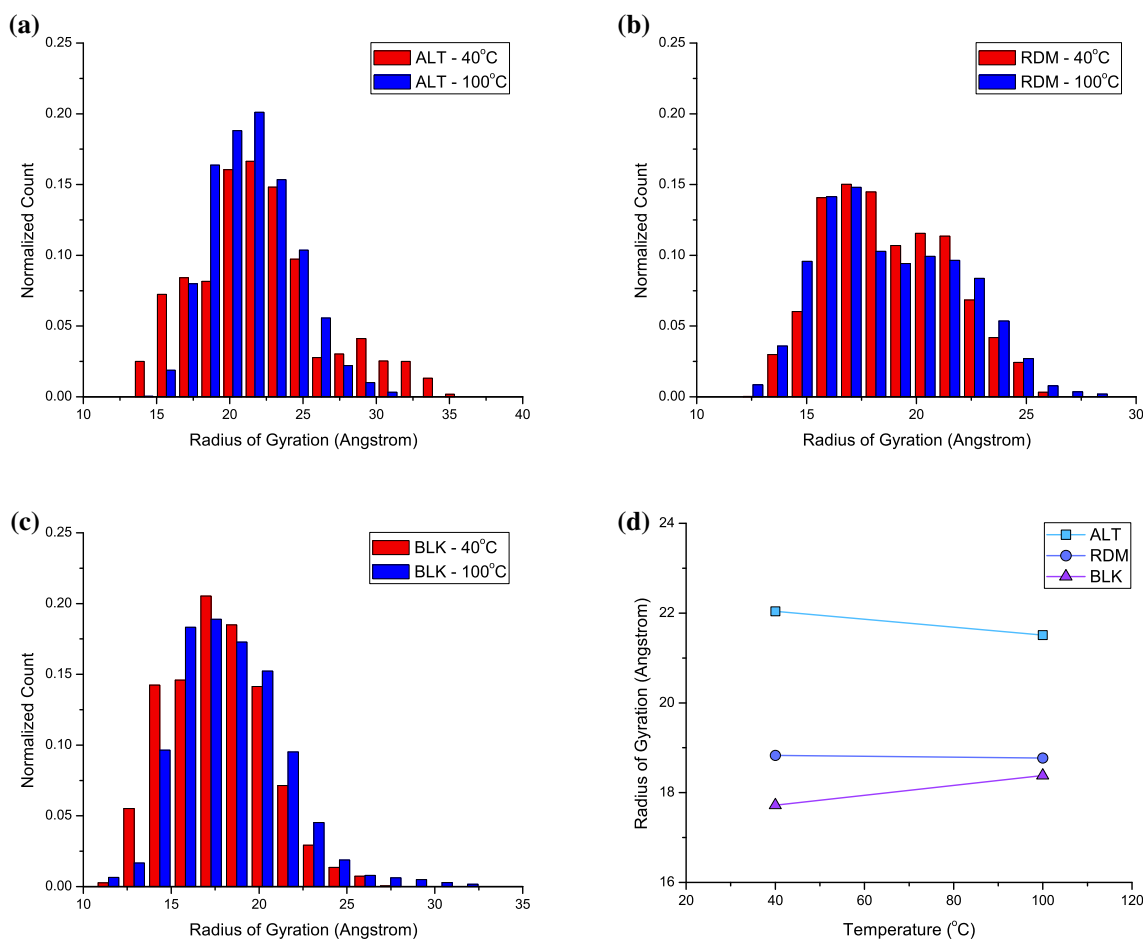
Fig. 4 Frequency histograms for the **a** ALT, **b** RMD and **c** BLK configurations at 40 and 100 °C. Gaussian functions are fit to these histograms to quantify the mean of the distribution. **d** Mean R_g versus temperature for all three SB configurations, where the lines connecting the symbols are just guides to the eye

Table 2 Mean and skewness of the R_g distribution for the SB configurations as well as the percent change in the coil size (R_g) with increased temperature

System	Mean			Skewness	
	40 °C (Å)	100 °C (Å)	% Change	40 °C	100 °C
ALT	22.0 ± 4.4	21.5 ± 2.9	−2.4	0.6	0.4
RDM	18.8 ± 2.8	18.8 ± 3.1	−0.3	0.3	0.3
BLK	17.7 ± 2.8	18.4 ± 3.0	3.7	0.3	0.8

Table 3 Number of contact pairs present in the polymer due to coiling at both temperatures and for all SB configurations

System	40 °C	100 °C
ALT	63 ± 10	68 ± 13
RDM	96 ± 13	97 ± 12
BLK	107 ± 17	106 ± 19

changes in viscosity with temperature. The BLK structure exhibits this behavior, due to the flexibility of the butadiene blocks.

4 Conclusions

The temperature–viscosity behavior of solutions containing linear styrene–butadiene polymers with alternating, random, and block configurations was investigated using MD simulation. The viscosity–temperature response of these configurations was characterized, as well as the mechanisms underlying that response. First, viscosity was calculated at a range of shear rates using RNEMD. The resultant data were fit to the Carreau equation to calculate the Newtonian viscosity of each model solution. The temperature–viscosity behavior of each fluid was quantified by its PVI, which showed that the BLK configuration exhibits the best performance. To understand this result, the radius of gyration and the intramolecular interactions of

each polymer model were characterized as functions of temperature. Small coil size and large number of contact pairs were correlated with good PVI. Of the three configurations studied, the block structure exhibited the least change in viscosity with temperature. This configuration was also observed to form small and tight coils with many intramolecular interactions at low temperatures and then expand as the temperature was increased. This observation suggests that structures that can attain very small conformations at the lower temperatures and expand as temperature is increased will function as ideal VII additives.

Overall, the results indicate that temperature–viscosity behavior is correlated to styrene–butadiene polymer structure because the structure determines the polymer's response to temperature. Further, the method proposed in this study can be applied to other chemistries to better understand the structure–property–function relationships that are key to additive functionality. Successful implementation may lead to the development of a molecular tuning tool which could redefine our understanding of fluid properties and facilitate the design of lubricants with optimal performance and functionality.

References

1. Bair, S., Qureshi, F.: The high pressure rheology of polymer-oil solutions. Tribol. Int. **36**(8), 637–645 (2003)
2. Simmons, G., Glavatskih, S.: Synthetic lubricants in hydrodynamic journal bearings: experimental results. Tribol. Lett. **42**(1), 109–115 (2011)
3. Jukic, A., Vidovic, E., Janovic, Z.: Alkyl methacrylate and styrene terpolymers as lubricating oil viscosity index improvers. Chem. Tech. Fuels Oils **43**(5), 386–394 (2007)
4. Mohamad, S.A., Ahmed, N.S., Hassanein, S.M., Rashad, A.M.: Investigation of polyacrylates copolymers as lube oil viscosity index improvers. J. Petrol. Sci. Eng. **100**, 173–177 (2012)
5. Jerbić, I.Š., Vuković, J.P., Jukić, A.: Production and application properties of dispersive viscosity index improvers. Ind. Eng. Chem. Res. **51**(37), 11914–11923 (2012)
6. Stöhr, T., Eisenberg, B., Müller, M.: A new generation of high performance viscosity modifiers based on comb polymers. SAE Int. J. Fuels Lubr. **1**(2008-01-2462), 1511–1516 (2008)
7. Morgan, S., Ye, Z., Subramanian, R., Zhu, S.: Higher-molecular-weight hyperbranched polyethylenes containing crosslinking structures as lubricant viscosity-index improvers. Polym. Eng. Sci. **50**(5), 911–918 (2010)
8. Wang, J., Ye, Z., Zhu, S.: Topology-engineered hyperbranched high-molecular-weight polyethylenes as lubricant viscosity-index improvers of high shear stability. Ind. Eng. Chem. Res. **46**(4), 1174–1178 (2007)
9. Ghosh, P., Das, M.: Synthesis, characterization, and performance evaluation of some multifunctional lube oil additives. J. Chem. Eng. Data **58**(3), 510–516 (2013)
10. Fan, J., Müller, M., Stöhr, T., Spikes, H.A.: Reduction of friction by functionalised viscosity index improvers. Tribol. Lett. **28**(3), 287–298 (2007)
11. Spikes, H.: Friction modifier additives. Tribol. Lett. **60**(5), 1–26 (2015)
12. Nunez, C.M., Chiou, B., Andrady, A.L., Khan, S.A.: Solution rheology of hyperbranched polyesters and their blends with linear polymers. Macromolecules **33**(5), 1720–1726 (2000)
13. Ishizu, K., Tsubaki, K., Mori, A., Uchida, S.: Architecture of nanostructured polymers. Prog. Polym. Sci. **28**(1), 27–54 (2003)
14. Knothe, G., Steidley, K.R.: Kinematic viscosity of biodiesel fuel components and related compounds. Influence of compound structure and comparison to petrodiesel fuel components. Fuel **84**(9), 1059–1065 (2005)
15. Gaciño, F.M., Regueira, T., Lugo, L., Comuñas, M.J.P., Fernández, J.: Influence of molecular structure on densities and viscosities of several ionic liquids. J. Chem. Eng. Data **56**(12), 4984–4999 (2011)
16. Kioupis, L.I., Maginn, E.J.: Molecular simulation of poly-olefin synthetic lubricants: impact of molecular architecture on performance properties. J. Chem. Eng. Data **103**(49), 10781–10790 (1999)
17. Bhattacharya, P., Ramasamy, U.S., Krueger, S., Robinson, J.W., Tarasevich, B.J., Martini, A., Cosimbescu, L.: Trends in thermoresponsive behavior of lipophilic polymers. Ind. Eng. Chem. Res. **55**(51), 12983–12990 (2016)
18. Khabaz, F., Khare, R.: Effect of chain architecture on the size, shape, and intrinsic viscosity of chains in polymer solutions: a molecular simulation study. J. Chem. Phys. **141**(21), 214904 (2014)
19. Covitch, M.J., Trickett, K.J.: How polymers behave as viscosity index improvers in lubricating oils. Adv. Chem. Eng. Sci. **5**(02), 134–151 (2015)
20. Selby, T.W.: The non-Newtonian characteristics of lubricating oils. ASLE Trans. **1**(1), 68–81 (1958)
21. Mary, C., Phillipon, D., Lafarge, L., Laurent, D., Rondelez, F., Bair, S., Vergne, P.: New insight into the relationship between molecular effects and the rheological behavior of polymer-thickened lubricants under high pressure. Tribol. Lett. **52**(3), 357–369 (2013)
22. Müller, H.G.: Mechanism of action of viscosity index improvers. Tribol. Int. **11**(3), 189–192 (1978)
23. LaRiviere, D., Asfour, A.F.A., Hage, A., Gao, J.Z.: Viscometric properties of viscosity index improvers in lubricant base oil over a wide temperature range. Part I: group II base oil. Lubr. Sci. **12**(2), 133–143 (2000)
24. Ramasamy, U.S., Lichter, S., Martini, A.: Effect of molecular-scale features on the polymer coil size of model viscosity index improvers. Tribol. Lett. **62**(23), 1–7 (2016)
25. Plimpton, S.: Fast parallel algorithms for short-range molecular dynamics. J. Comp. Phys. **117**(1), 1–19 (1995)
26. Jorgensen, W., Maxwell, D., Tirado-Rives, J.: Development and testing of the opls all-atom force field on conformational energetics and properties of organic liquids. J. Am. Chem. Soc. **118**(45), 11225–11236 (1996)
27. Nosé, S.: A unified formulation of the constant temperature molecular dynamics. J. Comp. Phys. **81**(1), 511–519 (1984)
28. Nosé, S.: A molecular-dynamics method for simulations in the canonical ensemble. Mol. Phys. **52**(2), 255–268 (1984)

29. Hoover, W.G.: Canonical dynamics: equilibrium phase-space distributions. Phys. Rev. A **31**(3), 1695–1697 (1985)

30. Ye, X., Cui, S., de Almeida, V.F., Khomami, B.: Effect of varying the 1–4 intramolecular scaling factor in atomistic simulations of long-chain n-alkanes with the opls-aa model. J. Mol. Model **19**(3), 1251–1258 (2013)

31. Müller-Plathe, F.: Reversing the perturbation in non-equilibrium molecular dynamics: an easy way to calculate the shear viscosity of fluids. Phys. Rev. E **59**(5), 4894–4898 (1999)

32. Kelkar, M.S., Rafferty, J.L., Maginn, E.J., Siepmann, J.I.: Prediction of viscosities and vapor-liquid equilibria for five polyhydric alcohols by molecular simulation. Fluid Phase Equilib. **260**(2), 218–231 (2007)

33. Tenney, C.M., Maginn, E.J.: Limitations and recommendations for the calculation of shear viscosity using reverse nonequilibrium molecular dynamics. J. Chem. Phys. **132**(1), 014103 (2010)

34. Jacobs, T.B.D., Martini, A.: Measuring and understanding contact area at the nanoscale: a review. Appl. Mech. Rev (2017)

35. Lemmon, E.W., McLinden, M.O. , Friend, D.G.: Thermophysical properties of fluid systems. In: Linstrom, P.J., Mallard, W.G. (eds.). NIST Chemistry WebBook, NIST Standard Reference Database Number 69. National Institute of Standards and Technology, Gaithersburg MD (retrieved August 17, 2017)

36. Zakarian, J.: The limitations of the viscosity index and proposals for other methods to rate viscosity-temperature behavior of lubricating oils. SAE Int. J. Fuels Lubr. **5**(2012-01-1671), 1123–1131 (2012)

37. Zempel, R.W.: Poly(Styrene-Butadiene). In: Tracton, A.A. (ed.) Coatings Technology Handbook, 3rd edn. CRC Press, Boca Raton (2005)